The EMBO Journal (2009) 28, 1392–1406 | © 2009 European Molecular Biology Organization | All Rights Reserved 0261-4189/09
www.embojournal.org

THE EMBO JOURNAL

MAPKAP kinase MK2 maintains self-renewal capacity of haematopoietic stem cells

Jessica Schwermann[1,4], Chozhavendan Rathinam[2,4,5], Maria Schubert[1,4], Stefanie Schumacher[1], Fatih Noyan[2], Haruhiko Koseki[3], Alexey Kotlyarov[1,4], Christoph Klein[2,4] and Matthias Gaestel[1,4,*]

[1]Institute of Biochemistry, Hannover Medical School, Hannover, Germany, [2]Department of Pediatric Hematology/Oncology, Hannover Medical School, Hannover, Germany and [3]RIKEN Research Center for Allergy and Immunology, Tsurumi-ku, Yokohama, Japan

The structurally related MAPK-activated protein kinases (MAPKAPKs or MKs) MK2, MK3 and MK5 are involved in multiple cellular functions, including cell-cycle control and cellular differentiation. Here, we show that after deregulation of cell-cycle progression, haematopoietic stem cells (HSCs) in MK2-deficient mice are reduced in number and show an impaired ability for competitive repopulation *in vivo*. To understand the underlying molecular mechanism, we dissected the role of MK2 in association with the polycomb group complex (PcG) and generated a MK2 mutant, which is no longer able to bind to PcG. The reduced ability for repopulation is rescued by re-introduction of MK2, but not by the Edr2-non-binding mutant of MK2. Thus, MK2 emerges as a regulator of HSC homeostasis, which could act through chromatin remodelling by the PcG complex.

The EMBO Journal (2009) **28,** 1392–1406. doi:10.1038/emboj.2009.100; Published online 16 April 2009
Subject Categories: signal transduction; differentiation & death
Keywords: chromatin remodelling; haematopoiesis; mouse knockout; protein kinase

Introduction

Haematopoietic stem cells (HSCs) represent the best-characterized type of adult stem cells. Profound analysis of surface antigens and established protocols to determine the self-renewal capacity and differentiation make HSCs a favourite model for stem cell biology. The complex microenvironment in the bone marrow regulates the fate of HSCs, controlling the balance between differentiation and self-renewal by providing cytokine and growth factors. However, intracellular signalling pathways involved in HSCs maintenance remain elusive. Recent studies showed controversial roles of evolutionarily conserved signalling pathways such as Smad-, Notch- and Wingless/Int(Wnt)-type (Reya *et al*, 2003; Duncan *et al*, 2005; Blank *et al*, 2006). The p38 mitogen-activated protein kinase (MAPK) pathway mainly regulates haematopoiesis by myelosuppressive cytokines that inhibit the growth of human primitive haematopoietic progenitors (reviewed in Platanias, 2003). p38 MAPK was also described to be necessary for erythropoietin expression and erythropoiesis (Tamura *et al*, 2000) and for thrombopoietin-induced self-renewal and expansion of HSCs through homeobox protein Hoxb4 (Kirito *et al*, 2003). More recently, the involvement of p38 MAPK in oxidative stress-elicited HSC depletion was shown (Ito *et al*, 2006). However, redundancy in these signalling pathways as well as the early embryonic lethality of most knockout mouse models makes the systemic analysis of the involvement of these pathways still puzzling.

The three MAPKAP kinases (MKs), MK2, MK3 and MK5, are involved in the regulation of inflammatory-cytokine production, in rearrangement of the cytoskeleton and cell migration, in cell-cycle checkpoint control, in developmental regulation, as well as in chromatin repression and remodelling (reviewed in Gaestel, 2006). Whereas the regulatory function of MKs in cytokine production is well known (Kotlyarov *et al*, 1999; Winzen *et al*, 1999), their role in controlling chromatin repression and remodelling remains elusive. Recent evidence indicates that polycomb group proteins may be targets for MK2 (Yannoni *et al*, 2004) and MK3 (Voncken *et al*, 2005). The polycomb group family, originally identified in *Drosophila melanogaster* as a repressor of homeotic genes, represents epigenetic chromatin modifiers with transcriptional silencing function (Zink and Paro, 1989; Valk-Lingbeek *et al*, 2004). In *Drosophila* and mammals, two cooperating PcG complexes have been identified (Lund and van Lohuizen, 2004). The polycomb repressive or initiation complex (PRC2), which shows histone-modifying activity, cooperates with the polycomb maintenance complex (PRC1), which interacts with modified histones to repress the expression of genes (Levine *et al*, 2004), such as the developmental regulators in murine embryonic stem cells (Boyer *et al*, 2006). In humans, PRC1 is a multiprotein complex including the human polycomb proteins HPC1–3, core proteins such as RING1A, RING1B, BMI1, as well as the early development regulator/human polyhomeotic EDR1/HPH1 and EDR2/HPH2. PcG proteins can interact with a series of additional molecules to exert control on gene expression in a highly regulated and dynamic manner (reviewed in Lund and van Lohuizen, 2004).

A crucial role of PRC1 and its individual components has been shown by analysis of mice with targeted deletion of mouse homologues of BMI1 (Bmi1), EDR1/HPH1 (Edr1/Mph1/Phc1/Rae28) and EDR2/HPH2 (Edr2/Mph2/Phc2). Bmi1-deficient mice are characterized by progressive

*Corresponding author. Institute of Biochemistry, Hannover Medical School, Carl-Neuberg-Str.1, 30625 Hannover, Germany.
Tel.: +49 511 532 2825; Fax: +49 511 532 2827;
E-mail: gaestel.matthias@mh-hannover.de
[4]These authors contributed equally to this work
[5]Present address: Department of Immunobiology, Yale University School of Medicine, New Haven, CT 06520, USA

Received: 10 October 2008; accepted: 24 March 2009; published online: 16 April 2009

loss of HSCs and cerebellar neurons (van der Lugt *et al*, 1994). More recently, direct evidence implicated Bmi1 in the self-renewal of stem cells (Lessard and Sauvageau, 2003; Molofsky *et al*, 2003; Park *et al*, 2003). Similarly, Mph1/Rae28-deficient HSCs show decreased proliferative and self-renewal capacity (Ohta *et al*, 2002; Park *et al*, 2003). In addition to defects in the homeostasis of HSCs, PRC1 and PRC2 PcG mutant mice also suffer from lymphoid differentiation defects (reviewed in Valk-Lingbeek *et al*, 2004) and, in case of Phc2/Edr2, from changes in skeleton and premature senescence (Isono *et al*, 2005). Thus, PcG proteins play a crucial role in regulating stem cell self-renewal and differentiation (recently reviewed in Rajasekhar and Begemann, 2007).

In vitro evidence indicates that MK2 and MK3 may selectively interact with EDR2/HPH2 and target components of PRC1 (Yannoni *et al*, 2004; Voncken *et al*, 2005), suggesting a functional link between MAPKAP kinases and polycomb proteins. Here, we analyse the interaction between mouse PRC1 and MK2 and unequivocally document a role for the MK2 complex in maintaining the 'stemness' of HSCs *in vivo*.

Results

Phenotypic characterization of haematopoietic stem cells of MK2−/− mice

To numerically assess HSCs, we first quantified the Lin-(CD3ε−, CD11b−, B220−, Gr-1−, TER119−)-Sca1 + c-Kit + (LSK) population, classically defined as the HSC compartment. Compared with wild-type mice cells, LSK cells appeared to have increased in relative and absolute numbers in MK2−/− mice (Figure 1A and B). As LSK cells contain LT-HSC, ST-HSC, ELPs and multipotent progenitors, we also analysed HSCs defined by expression of SLAM family receptors (Kiel *et al*, 2005). As shown in Figure 1B and C, MK2−/− mice showed a decrease in CD150 + CD48− cells compared with wild-type control mice. Furthermore, upon staining total bone marrow with the Hoechst dye 33342, MK2−/− mice showed a five-fold reduction in side population (SP) cells, known to contain quiescent HSC (Goodell *et al*, 1996) (Figure 1D). LSK cells were further analysed for expression of CD34 and Flt3 to differentiate long-term (LT) (CD34−Flt3−)-, short-term (ST) (CD34 + Flt3−)-HSCs and multipotent progenitor cells (MPPs)(CD34 + Flt3 +). The relative proportion and absolute number of LT-HSCs are decreased in MK2−/− mice whereas these values are increased for MPPs (Figure 1E and F). To assess whether the lack of MK2 has any effects on the differentiation of HSC, we analysed erythroid, myeloid, and lymphoid cells in the bone marrow and spleen. In consistence with the results published earlier (Kotlyarov *et al*, 1999), the proportions of TER119, CD11b and Gr1 were not different between MK2−/− and control mice; furthermore, no differences were seen in phenotypic studies characterizing common lymphoid and myeloid progenitor cells (Supplementary Figures 1–5). In addition, by blood cell count we could not detect a haematopoietic failure in 4-, 8- and 12-months old mice, thus confirming data published earlier (Hegen *et al*, 2006; Jagavelu *et al*, 2007). These findings indicate that the HSC pool is significantly reduced in MK2−/− mice, whereas differentiation of HSCs and progenitor cells is not affected.

Functional characterization of MK2-deficient HSC

We hypothesized that inefficient PcG-mediated transcriptional repression may lead to a release of the actively maintained state of quiescence in HSC. This, in turn, should be associated with increased proliferative responses of HSCs to cytokines. To directly measure the HSC proliferation, we isolated LSK cells from wild-type and MK2−/− mice and cultured them in the presence of a recombinant cytokine cocktail consisting of SCF, IL3, IL6, Flt3L and TPO. As expected, MK2−/− LSK cells showed a significantly higher proliferative response as assessed by ^{3}H-thymidine incorporation (Figure 2A). We were also interested in monitoring the proliferation of different HSC sub-populations in the absence of cytokine stress *in vivo*. MK2−/− and wild-type mice were fed with BrdU for 48 h, and the BrdU incorporation into LSK cells was determined by FACS analysis. MK2−/− LT-, ST-HSCs and MPPs showed increased staining for BrdU (Figure 2B), indicating that enhanced proliferation of HSC is not only associated with cytokine exposure *in vitro* but also occurs in the physiological bone marrow environment *in vivo*.

To further assess a putative state of promoted cell-cycle progression in LSK cells, we carried out cell-cycle analysis using propidium iodide staining of *in vitro*-cultured LSK cells as well as LSK cells directly prepared from mice. In comparison with wild-type cells, MK2−/− cells showed fewer cells in G1/G0 phase and more cells in S and G2/M phases (Figure 2C), thus confirming increased cell-cycle progression in the absence of MK2. Cyclin-dependent kinase inhibitors are important mediators of cell quiescence and serve as checkpoints, restricting cell-cycle transition. P21Cip1Waf1-deficient HSCs show impaired self-renewal and increased proliferation (Cheng *et al*, 2000). To determine the expression levels of P21Cip1Waf1, we carried out RT–PCR analysis in CD150 + CD48− HSCs from MK2−/− and wild-type mice. As shown in Figure 2D, MK2−/− CD150 + CD48− HSCs show decreased abundance of p21Cip1/Waf1 mRNA, a finding in line with accelerated cell cycle progression in MK2−/− cells. Similar findings of decreased p21 mRNA level and increased cell-cycle progression were reported in Gfi1-deficient HSCs (Hock *et al*, 2004). To shed light on the molecular mechanism of reduced stem-cell quiescence, we determined expression levels of direct downstream targets of Bmi1, p16Ink4a and p19Arf. In the absence of Bmi1, repression of the Ink4a locus is relieved, resulting in expression of p16Ink4a and p19Arf (Jacobs *et al*, 1999). As shown in Figure 2E, MK2-deficient CD150 + CD48− HSCs show higher expression levels of p19Arf, whereas the expression levels of Ink4a and p27 (Kip1) were comparable to those of wildtype control cells (data not shown).

Cytokine-induced proliferation of HSC *in vitro* is associated with loss of 'stemness'. We hypothesized that the sequence of events resulting in loss of stemness might occur more rapidly in unrestricted proliferation of MK2-deficient HSC. As no phenotypic marker unequivocally reflects HSC function, we monitored the cell-surface expression of Sca1 as a surrogate parameter for early haematopoietic progenitor activity. CD150 + /CD48− HSCs from MK2−/− and wild-type mice were sorted (Figure 3A, upper panel) and cultured *in vitro* in the presence of the recombinant cytokines SCF, IL3, IL6, Flt3L, and TPO. Immediately after cell sorting, both MK2−/− and wild-type CD150 + /CD48− HSCs showed an

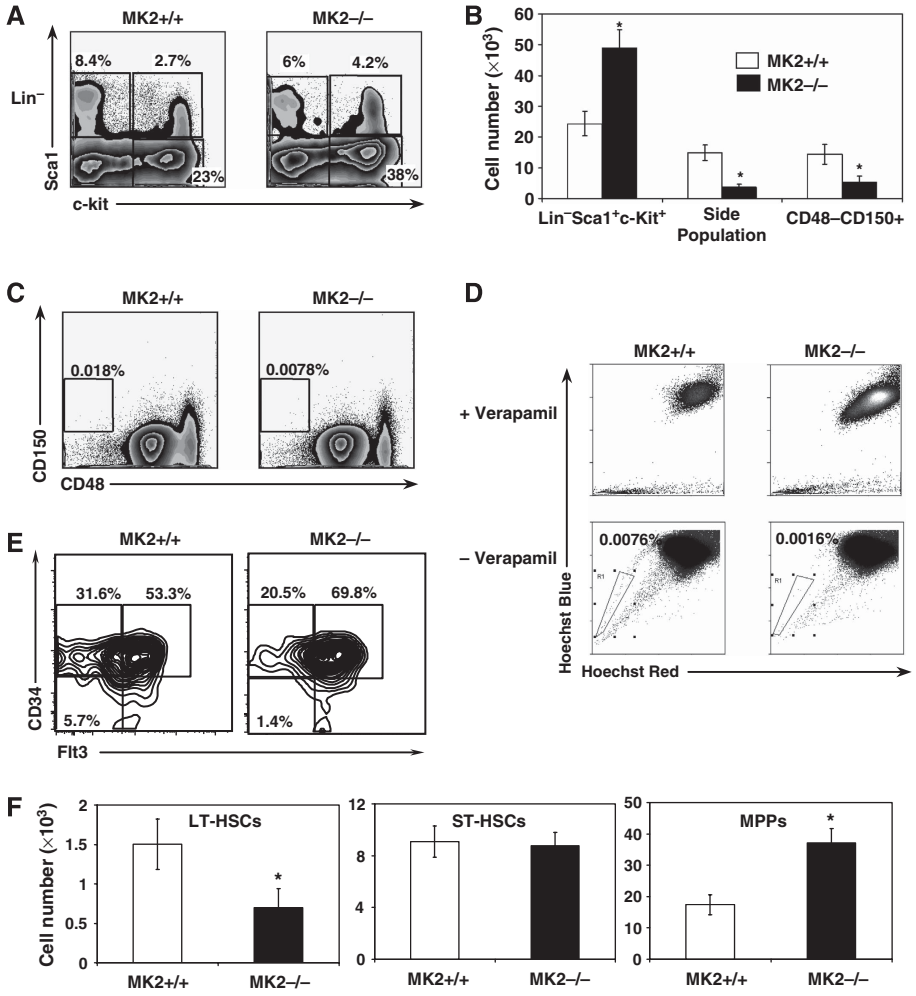

Figure 1 Phenotypic analysis of the haematopoietic stem cell compartment in MK2−/− mice. (**A**) FACS plots indicating relative increase of LSK cells in MK2−/− mice. Lineage-marker (CD3ε, CD11b, B220, Gr-1, TER119)-negative cells were gated and further analysed for expression of Sca1 and c-Kit. Data are representative of three independent experiments. (**B**) Absolute numbers of LSK, SP and CD150+ CD48− cells determined from the bone marrow of both hind limbs ($N=6$ mice). Data are representative of two independent experiments. Asterisks indicate statistical significance ($P<0.01$). (**C**) FACS plots indicating reduced frequency of CD150+ CD48− cells in MK2−/− mice. Data are representative of two independent experiments. (**D**) Side population (SP) analysis upon staining of BM cells with Hoechst 33342 dye. Cells stained with Hoechst 33342 dye in the presence of verapamil serve as controls for the specificity of the SP population. Data are representative of two independent experiments. (**E**) FACS plots indicating relative decrease of long-term (LT)-HSCs (CD34–Flt3–LSK) and short-term (ST)-HSCs (CD34+Flt3–LSK), and increase of multipotent progenitor cells (MPPs) (CD34+Flt3+LSK) in MK2−/− mice. Total BM cells of MK2+/+ and MK2−/− were prepared and stained with an antibody cocktail that recognizes lineage markers (CD11b, Gr1, B220, CD3e, TER119), Sca1 and c-Kit, and analysed by flow cytometry. LSK cells were pre-gated and further analysed for CD34 and Flt3 expression. (**F**) Absolute numbers of LT-HSCs (left), ST-HSCs (middle) and MPPs (right) determined from the bone marrow of both hind limbs ($N=5$ mice). Asterisks indicate statistical significance ($P<0.05$). Data in (E) and (F) are representative of three independent experiments.

equal pattern of expression of c-Kit and Sca1 (Figure 3A, middle panel). However, after 3 days *in vitro*, only between 16–21% of MK2−/− progenitor cells stained positive for Sca1, whereas between 60–75% of wild-type progenitor cells maintained Sca1 expression (Figure 3A, lower panel and quantification below), suggesting that MK2 is crucial for the maintenance of an early state of differentiation or quiescence. Similar results were obtained for LSK cells (data not shown). To assess whether cytokine-stimulated HSCs showed a skewed differentiation, we analysed the expression of lineage-specific cell surface markers. In comparison to wildtype cells, a larger fraction of MK2-deficient cells showed expression of CD11b and Gr1 (Supplementary Figures 6 and 7). Analysis of CD150+/CD48− HSCs using a CFSE dilution assay indicates higher proliferation of MK2-deficient cells (Figure 3B) similar to LSK cells (Figure 2A–C).

The *in vitro* culture system described above allowed us to test whether a direct inhibitor of p38 MAPK signalling similarly unleashes HSC quiescence. Wild-type LSK cells were purified and incubated for 48 h in the absence or presence of 5 μM SB239063, which does not reduce the overall viability of the cells (Supplementary Figure 8). As shown in Figure 3C, cells exposed to a specific p38 inhibitor almost completely lost the expression of Sca1, whereas cells stimulated in the absence of SB239063 remained largely positive for expression of Sca1. These findings corroborate the idea that p38 signalling is crucial for the maintenance of HSC quiescence.

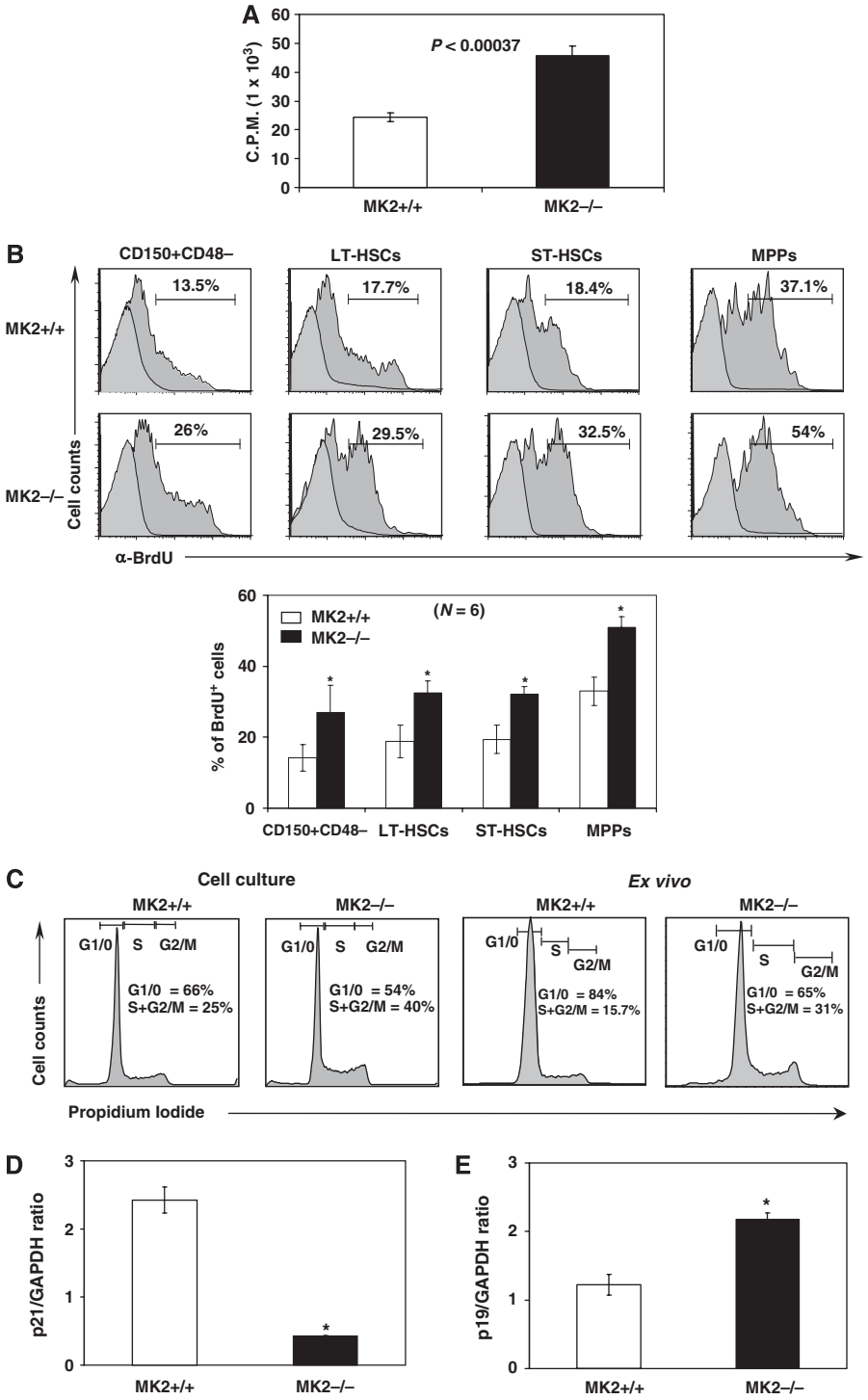

Figure 2 Increased proliferation of LSK in MK2−/− mice. (**A**) *In vitro* proliferation assay. Purified LSK cells were cultured in the presence of recombinant cytokines for 48 h, pulsed with ^{3}H-thymidine, and subjected to scintillation counting. The mean values of triplicate samples are shown. (**B**) *In vivo* BrdU incorporation experiment. The *in vivo*-proliferation potential of CD150 + CD48− cells, LT-HSCs, ST-HSCs and MPPs in MK2 + / + and MK2−/− mice was measured after feeding BrdU through drinking water for 2 days. RBC-depleted BM cells were stained with monoclonal antibodies recognizing subsets of HSCs and BrdU (negative controls of cells from mice fed with PBS are shown as insets in light grey). Indicated HSC subsets were pre-gated and histograms were generated for quantifying the incorporated BrdU (% of BrdU-positive cells is given). Data are representative of two independent experiments. Cells from three mice from each of the two experiments were measured separately ($N = 6$). Mean and statistics are in the diagram given below (asterisks indicate significant differences with $P < 0.05$). (**C**) Cell-cycle analysis. Purified LSK cells were cultured *in vitro* in the presence of recombinant cytokines for 48 h. Cells were fixed, stained with propidium iodide and their DNA content was measured by flow cytometry (left panel). LSK cells isolated from MK2 + / + and MK2−/− mice were sorted, directly fixed and stained with propidium iodide, and their DNA content was measured by flow cytometry (right panel). (**D**, **E**) Real-time PCR showing p21Cip1/Waf1 (D) and p19Arf mRNA levels (E) in purified CD150 + CD48–HSCs. The mean values of duplicate samples are shown. Asterisks indicate statistical significance ($P < 0.01$). Data are representative of two independent experiments each.

To directly assess the self-renewal capacity of HSC, we carried out competitive repopulation experiments. Various numbers of wild-type and MK2−/− bone marrow cells (CD45.2) were mixed with 10^5 wild-type CD45.1 competitor cells and transplanted into lethally irradiated CD45.1 recipient mice. Three months later, the mice were killed and the specific contribution of CD45.1 and CD45.2 cells to haematopoiesis was assessed by FACS analysis. In line with earlier experiments (Kotlyarov *et al*, 1999) and the data shown in Supplementary Figures 1–5, no defect of differentiation in various haematopoietic lineages could be observed in mice transplanted with MK2−/− cells (data not shown), confirming that MK2 is not crucially involved in controlling HSC differentiation. When 10^5 HSCs were mixed with 10^5 competitor cells, MK2-deficient cells contributed to 54% of haematopoiesis, whereas wild-type cells contributed to 75% of haematopoiesis. However, under limiting conditions, when fewer HSCs were transplanted, the statistically significant

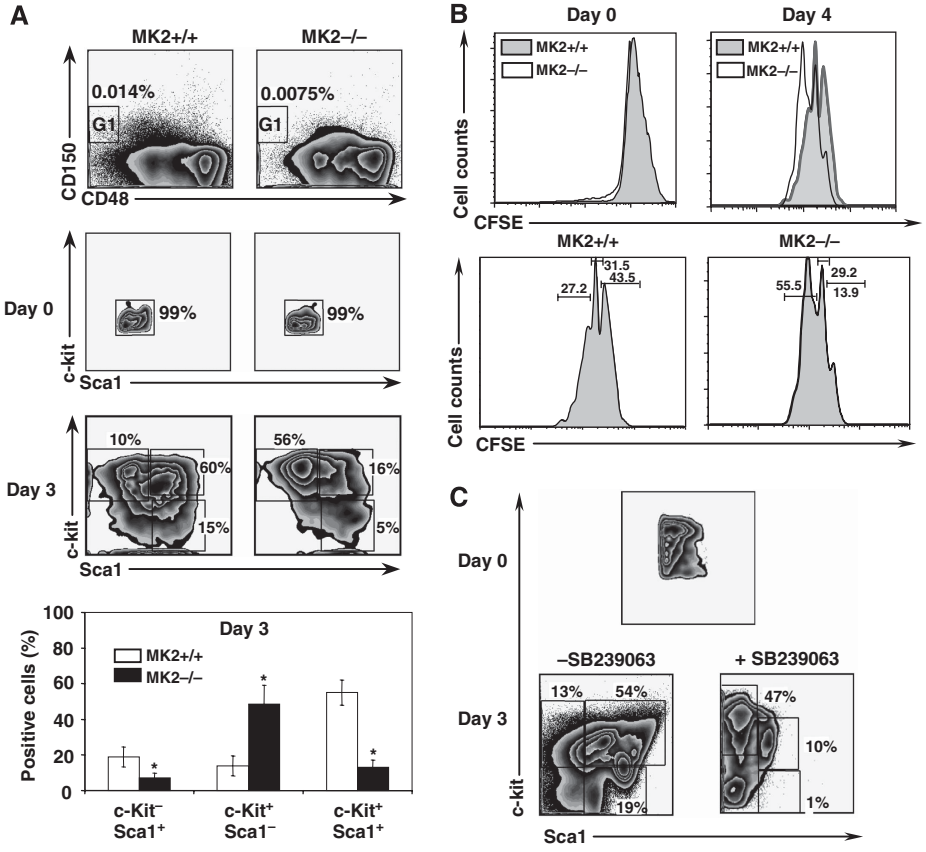

Figure 3 Compromised haematopoietic stem cell function in MK2−/− mice. (**A**) Contour plots indicating an accelerated loss of Sca1 expression in MK2−/− SLAM cells *in vitro*. The upper panel shows sorting of SLAM cells, the middle panel shows expression pattern of Sca1 and c-Kit in primary sorted SLAM cells; and the two lower panels show Sca1 and c-Kit expression after 3 days of *in vitro* culture in the presence of recombinant cytokines. Cell subsets were discriminated on the basis of differential expression of Sca1 and c-Kit, their percentages were calculated and plotted. Asterisks indicate statistical significance ($P<0.01$). Data are representative of two independent experiments. (**B**) CFSE-proliferation assay for WT and MK2-deficient SLAM cells. Sorted CD150+CD48− HSCs of MK2+/+ and MK2−/− mice were stained with CFSE and cultured *in vitro* in the presence of cytokine cocktail for 3 days. On day 4, aliquots of cells were analysed by flow cytometry. Histograms, documenting increased *in vitro* proliferation of MK2−/− CD150+CD48− HSCs, as assessed by the percentage of cells that appear under gates that measure each cycle of proliferation. (**C**) FACS plots indicating an accelerated loss of Sca1 expression in MK2+/+ cells in the presence of the MAPK p38 inhibitor SB239063. The upper panel shows the expression pattern of Sca1 and c-Kit in primary sorted LSK cells, lower panels show Sca1 and c-Kit expression after 3 days *in vitro* culture containing recombinant cytokines in the presence or absence of SB239063, respectively. Data are representative of two independent experiments. (**D**) Competitive repopulation experiment. 10^5 CD45.1$^+$ competitor BM cells were mixed with defined numbers of CD45.2+ MK2+/+ or CD45.2+ MK2−/− BM cells, and total BM was analysed for competitive repopulation as described. A characteristic experiment (left) and statistical evaluation (right) ($N=5$) are shown. Asterisks indicate statistically significant ($P<0.05$, single sided *t*-test) differences between MK2-deficient and wildtype cells. (**E**) Competitive repopulation assay as in (D), but using 10^4 CD45.1+ competitor LSK cells mixed with defined numbers of CD45.2+ MK2+/+ or CD45.2+ MK2−/− LSK cells in lethally irradiated (9.5 Gy) CD45.1+ congenic recipients. A characteristic experiment (left) and statistical evaluation (right) ($N=10$) are shown. Asterisks indicate statistically significant ($P<0.05$, single-sided *t*-test) differences between MK2-deficient and wildtype cells. (**F**) Secondary transplantation of 2×10^6 WT and MK2−/− bone marrow cells (CD45.2) mixed with 10^5 competitor cells. Analysis was performed 16 weeks after transplant. A characteristic experiment (left) and statistical evaluation (right) ($N=5$) are shown. Asterisks indicate statistically significant ($P<0.05$, single-sided *t*-test) differences between MK2-deficient and wildtype cells. (**G**) FACS plots and quantification indicating reduced frequencies of CD150+CD48− HSCs in CD45.1 WT congenic recipients that received MK2−/− LSK cells. Sorted LSK (CD45.2) cells of MK2+/+ and MK2−/− mice were transplanted into lethally irradiated CD45.1 wildtype recipients. At 16 weeks after transplantation, donor-derived (CD45.2) haematopoietic cells of BM were pre-gated and analysed for CD150 and CD48 expression (left). Absolute numbers of donor (CD45.2)-derived CD150+ CD48− cells were determined from the bone marrow of both hind limbs ($N=5$ mice). The asterisk indicates statistically significance ($P<0.05$). Data are representative of two independent experiments.

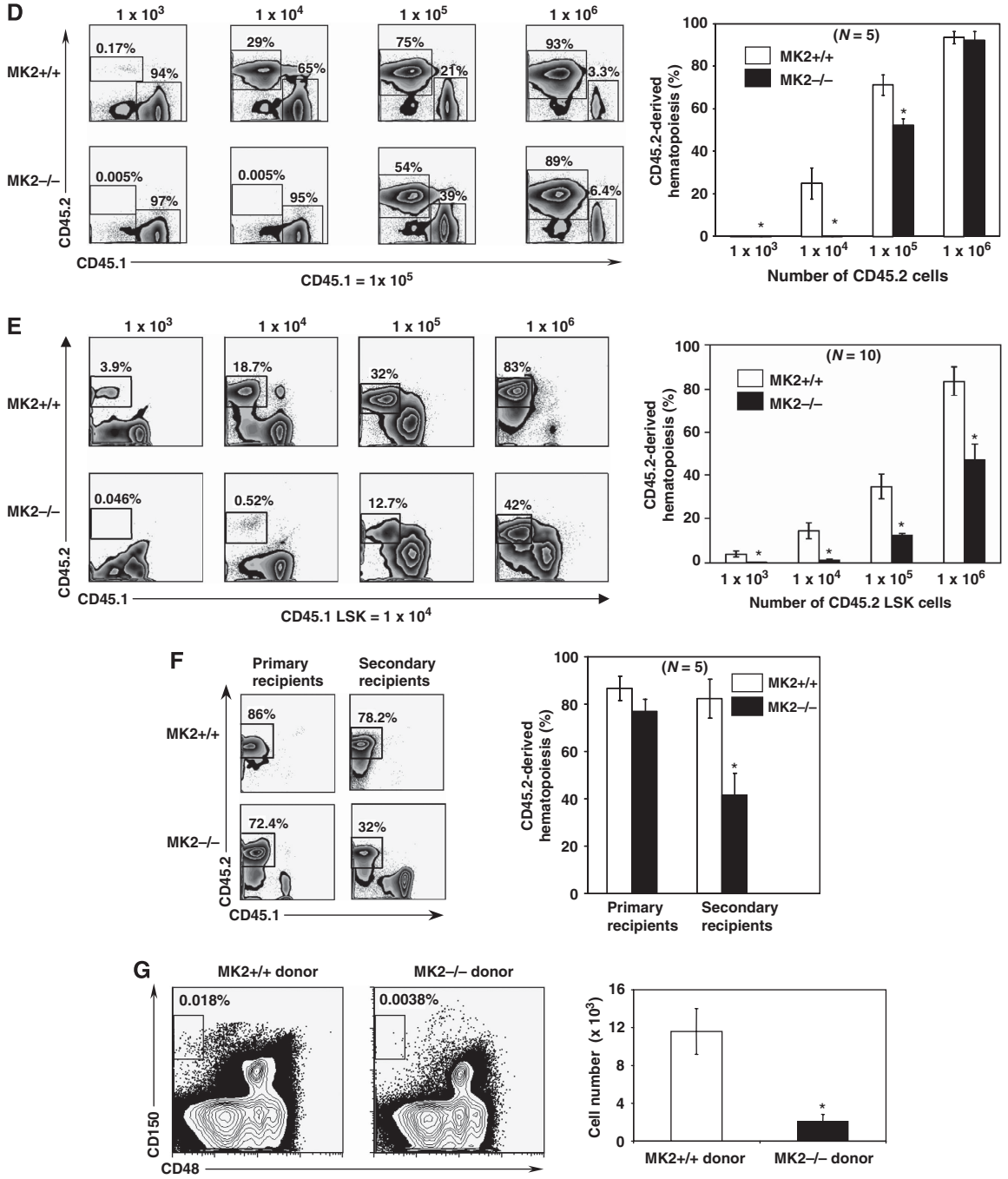

Figure 3 Continued.

difference between MK2-deficient cells and wildtype cells was striking (0.005 versus 29% for 10^4 HSCs and 0.005 versus 0.17% for 10^3 HSCs) (Figure 3D). Hence, MK2−/− HSCs showed an obvious disadvantage in their repopulation capacity, when compared with wild-type cells. To confirm and to further extend this finding, the repopulation experiment was also carried out with the LSK cell fraction enriched in HSCs. A similar defect was observed with respect to the LSK-repopulation capacity of MK2−/− cells (Figure 3E). We also carried out a secondary transplant experiment to confirm the self-renewal capacity of HSCs. Mice transplanted with a cell population of 2×10^6 WT and MK2−/− bone marrow cells (CD45.2) mixed with 10^5 competitor cells showed a mild reduction of CD45.2-positive MK2−/− cells compared with WT cells 12 weeks after transplantation (Figure 3F, primary recipients). When 2×10^6 bone marrow cells of these primary recipients were transplanted into secondary recipients, a defect of MK2−/− HSC became manifest (32% CD45.2 MK2−/− cells versus 78% CD45.2 MK2+/+ cells) (Figure 3F, secondary recipients), almost independently of addition of wild-type competitor cells (Supplementary Figure 9). Finally, the restoration of the CD150+CD48− HSC compartment after transplantation into WT mice, depending on the genotype of the donor cells, was analysed and was shown to be reduced for MK2-deficient donor cells (Figure 3G). Together these experiments show that a decreased quiescent

HSC pool in MK2−/− mice results in functional impairment under stress conditions.

Identification of Edr1 and Edr2 as interaction partners of MK2

To identify new interacting proteins for mouse MK2, a yeast-two-hybrid screen was carried out using a murine day-11-embryo brain library. The analysis revealed 27 positive clones: three of them carried cDNAs of the known MK2-interaction partner p38α, 17 clones carried 11 different cDNA fragments coding for C-terminal parts of mouse Edr1 ($n=4$), p36-Edr2 ($n=6$) and p90-Edr2 (Yamaki *et al*, 2002) ($n=1$). Interestingly, all Edr1/2 clones contained a single zinc-finger domain with the FCS signature followed by the region coding for the C-terminal homology domains (HD) II and III. HDII is also known as a sterile alpha motif (SAM) domain that has been shown to self-associate, bind to other SAM domains or form heteromeric interactions with some non-SAM domains of other proteins (Qiao and Bowie, 2005). The specificity of MK2–Edr1/2 interaction was confirmed by GST-pull-down experiments upon recombinant expression in *Escherichia coli*, using His–p38α/GST–MK2 interaction as a positive control. As shown in Figure 4A, His-Edr1 and His-Edr2 specifically bind to GST-MK2 but not to GST. In subsequent experiments, we limited our investigations to Edr2 interactions, as ectopic overexpression of Edr1 in mammalian cells was inefficient and available antibodies showed a low degree of specificity. Specific interaction of MK2 with endogenous Edr2 was shown by GST pull-down of endogenous Edr2 from HEK293-T cells transfected with different GST constructs (Figure 4B). Although endogenous Edr2 was found to bind to GST-MK2 and to the GST fusion of the structurally closely related MK3, which is expressed in LSK cells at levels comparable to MK2 (Supplementary Figure 10), as well as to the PcG member GST–Bmi1—used here as a positive control, GST fusion of the structurally more distant MK5, GST-MK5, was not able to bind Edr2 efficiently. We then extended the analysis of MK2–Edr2 interaction by carrying out co-immunoprecipitation of endogenous MK2 and Edr2 from mouse embryonic fibroblasts (Figure 4C). The specificity of the positive signal is shown by inefficient co-immunoprecipitation from lysates of MK2/3-deficient fibroblasts.

MK2 interacts with PRC1

Next, we were interested to know whether MK2 interacts with Edr2 within the physiological PRC1 complex. To this end, we tried to detect another core component of PRC1, the ring finger protein Ring1B, in the protein fraction bound to GST-MK2. As a negative control, we used again a GST-MK5 pull-down. As shown in Figure 4D, MK2, but not MK5, precipitates Ring1B, supporting the notion that MK2 is able to interact with the physiological PRC1 complex. To rule out the possibility that this interaction is because of the ectopic overexpression of the recombinant fusion proteins, we analysed the co-existence of the endogenous proteins in high molecular-weight fractions from lysates of mouse embryonic fibroblasts (MEFs). Lysates were separated by gel filtration and protein fractions were analysed by western blot using antibodies against Ring1B and MK2 (Figure 4E). In lysates from wildtype MEFs, co-separation of Ring1B and a small sub-population of MK2 can be detected in a fraction corresponding to a molecular mass of about 1MDa (asterisk). To show the specificity of the bands for MK2, we repeated this analysis with lysate from MK2-deficient MEFs. Although Ring1B can be detected in the corresponding fraction, the two corresponding bands for MK2 (boxed) are missing. This supports the notion that a sub-population of endogenous MK2 exists in the 1-MDa fraction, reflecting its interaction with endogenous PRC1. This interaction obviously does not include p38 MAPK, as it cannot be detected in the 1-MDa fraction (data not shown).

Edr2 and MK2 co-localize in polycomb bodies characteristic for PRC1

MK2 and p38α exist as a complex in the nucleus of resting cells. Upon activation of the p38 MAPK cascade, MK2 is phosphorylated, activated, and because of de-masking of a nuclear export signal, translocates to the cytoplasm (Ben-Levy *et al*, 1998; Engel *et al*, 1998; Neininger *et al*, 2001). In view of this finding, we hypothesized that a physiologically relevant nuclear PRC1–MK2 interaction may be released upon activation of the p38 MAPK cascade. First, we analysed the sub-cellular localization of MK2 and Edr2 in quiescent HEK293 cells upon transfection with MK2–YFP and Edr2–CFP fusion constructs. Both proteins showed perfect co-localization in speckles in the nucleus (polycomb bodies), reminiscent of the characteristic distribution pattern of proteins organized in PRC1 complexes such as endogenous Edr1, Edr2, Bmi1 and Ring1B (Suzuki *et al*, 2002) (Figure 5A). Second, we visualized stress-dependent translocation of GFP-MK2 in HeLa cells co-transfected with HA-Edr2. In contrast to our hypothesis, arsenite-induced stress activation of the p38 MAPK cascade did not trigger complete translocation of MK2 into the cytoplasm. In strict dependence on Edr2 co-expression, a sub-fraction of MK2 was retained in the polycomb bodies (Figure 5B), suggesting that activated MK2 alone or in complex with p38 may also have a physiological function at the nuclear PRC1 (cf. also schematic presentation of Figure 7).

Identification of the Edr2-interacting region in MK2

To further dissect the molecular interaction between MK2 and Edr2, we carried out GST–Edr2 pull-down assays using GFP fusion proteins with defined MK2 subdomains. Two regions of the small lobe of the kinase, subdomains I–III (amino acids 29–99) and IV-V (amino acids 97–131), are sufficient to interact with Edr2 (Figure 6A and B), indicating that both regions contribute to the interaction. The specific role of these subdomains for interacting with Edr2 was further substantiated using a MK2/MK5 hybrid molecule. When amino acids 38–128 are replaced by the homologous region of MK5, the hybrid molecule no longer binds to Edr2, as shown in pull-down experiments (Figure 6C), as well as in the co-localization assay (Figure 6D). As these domains do not overlap with the C-terminal docking site for p38α at amino acids 371–375 (Tanoue *et al*, 2000), it is possible that MK2, Edr2 and p38 can form a ternary complex at PRC1.

Functional rescue of MK2-deficient HSCs requires Edr2-binding of MK2

Finally, we were interested to determine a direct functional link between the HSC phenotype of MK2−/− mice and the Edr2-binding properties of MK2. To address this issue, we made use of the MK2/5 hybrid molecule, which is unable to

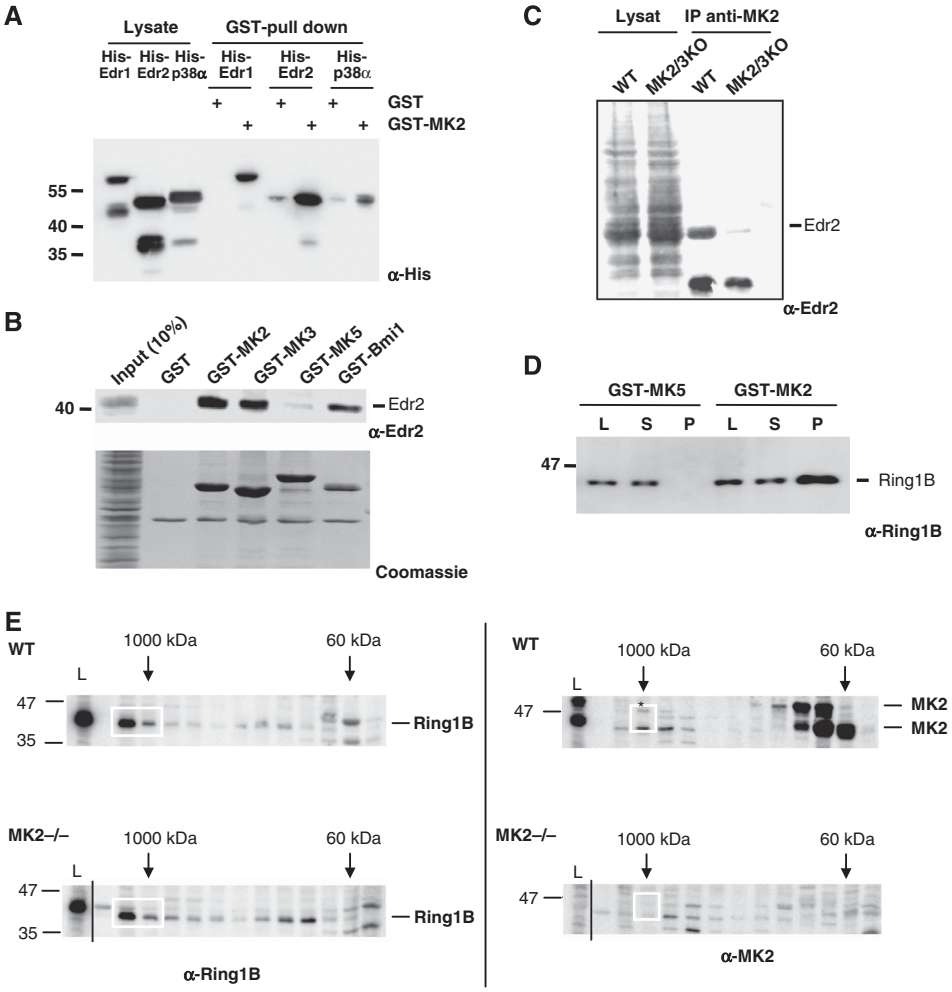

Figure 4 Interaction of MK2 with PRC1 components. (**A**) MK2 interaction with recombinant Edr1 and Edr2 *in vitro*. GST pull-down (right) of recombinant 6-His-tagged Edr1/2 from *E. coli* lysate. As a positive control, 6-His-tagged p38α is used; as negative control pull-down is performed with GST alone. Total *E. coli* lysates are separated at the left. His-tagged proteins are detected by anti-hexahistidine western blot. (**B**) Interaction of MK2 with endogenous Edr2. Whole-cell lysate of transfected HEK 293-T cells were used in a GST pull-down with recombinant GST-MK2, GST-MK3, GST-MK5, GST (negative control) and GST-Bmi1 (positive control). Comparable expression and GST pull down of the fusion proteins was monitored by Coomassie protein staining. Specific interactions of GST-MK2, GST-MK3 and GST-Bmi1 with endogenous Edr2 were detected by western blot using Edr2 antibodies. (**C**) Co-IP of endogenous MK2 and Edr2 from WT mouse embryonic fibroblasts (MEFs) but not from MK2/3-deficient (MK2/3 KO) MEFs (negative control). (**D**, **E**) MK2 interaction with the PRC1 complex. (D) Lysates (L) from HEK 293 cells overexpressing Edr2 were subjected to GST pull-down using GST-MK2 and, as negative control, GST-MK5. Supernatant (S) and pull-down (P) were analysed for PRC1 complexes by western blot against the PRC1 component Ring1B. (E) Co-separation of endogenous Ring1B and endogenous MK2 in a high-molecular-weight fraction. Nuclear extracts from wildtype (WT) and MK2-deficient MEFs (MK2−/−) were applied to FPLC gel filtration using a Superose 6 HR 10/30 column. Proteins from load (L) and fractions were subsequently separated by SDS–PAGE. In both lower panels, an empty lane between load and fractions was cut out from the blot to align corresponding molecular-weight fractions between the analysis of WT (upper panel) and MK2-deficient (lower panel) cells. Ring1B and MK2 were detected by western blot. The approximate size of the native proteins in the chromatographic fractions is indicated on the top. The protein size in SDS–PAGE is indicated left. The Ring1B band and the two MK2-specific bands are indicated at the right of each blot. The bands representing the sub-population of MK2 in the high-molecular-weight fraction are marked by a box with asterisk in the anti-MK2 blot of separation of WT lysate. The corresponding region of separation of MK2-deficient lysate lacking these bands is also boxed. The MK2 antibody decorates also several bands in the lysate of MK2-deficient cells (MK2−/−) probably because of cross-reaction with MK3 and because of non-specific binding.

associate with Edr2 (see Figure 6C and D) but maintains full catalytic kinase activity, as shown in MK2/3 double knockout cells (Figure 6E). MK2/3 double-knockout embryonic fibroblasts do not display any stress-induced Hsp25 phosphorylation. In contrast, retrovirus-mediated expression of MK2/5 and MK2 yielded a comparable level of Hsp25 phosphorylation upon UV stimulation. Hence, MK2 and MK2/5 are indistinguishable with respect to their kinase activity and differ only in Edr2 binding, allowing the dissection of kinase function from Edr2-mediated effects in the MK2/5 hybrid kinase. We hypothesized that MK2-deficient cells would be reconstituted by MK2 but not by the MK2/5 hybrid kinase with respect to stem-cell fitness.

The viral constructs were then used to introduce MK2 and MK2/5 into lineage-marker negative MK2-deficient CD45.2 cells, yielding similar transduction rates (30%) as assessed by expression of the marker gene GFP. 10^4 bi-cistronic expression construct-transduced CD45.2 MK2-deficient LSK cells were mixed with the same number of control GFP-construct-transduced CD45.1 LSK WT competitor cells, transplanted into lethally irradiated CD45.1 recipient mice, which were analysed 3 month later. As seen in Figure 6F,

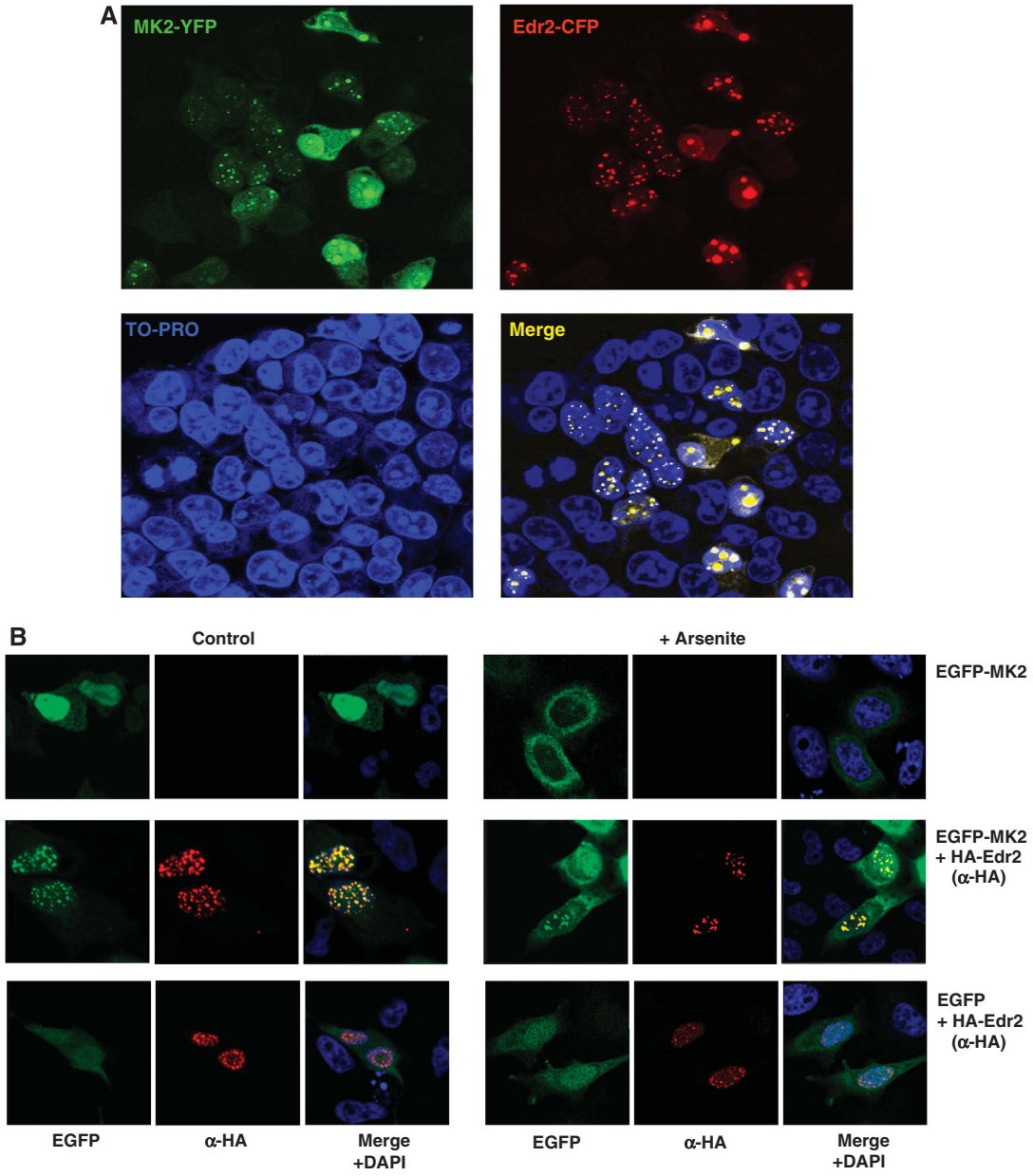

Figure 5 Co-localisation of MK2 and Edr2 in polycomb bodies characteristic for PRC1. (**A**) HEK 293 cells were transfected with constructs coding for an MK2-yellow fluorescent protein (YFP) fusion and an Edr2-CyAn fluorescent protein (CFP) fusion. Fusion proteins were visualized by fluorescence microscopy. Nuclei were stained using TO-PRO. (**B**) Stress-dependent changes in subcellular localizations of a GFP–MK2 fusion protein (GFP-MK2) in HeLa cells in the absence and presence of HA-tagged Edr2 (HA-Edr2). In the absence of HA-Edr2, arsenite treatment (+Arsenite) leads to export of evenly distributed GFP-MK2 from the nucleus. In cells overexpressing HA-Edr2 (+HA-Edr2), GFP–MK2 accumulates in polycomb bodies already before stress treatment (−Ars). Upon stress and in the presence of HA-Edr2, MK2 is translocated to the cytoplasm, but a sub-population of MK2 remains in polycomb bodies.

the LSK repopulation capacity of MK2−/− cells (6.8% in experiment 1 ($N=3$); 4.1% in experiment 2 ($N=3$)) is significantly increased by re-introduction of MK2 (42 and 49%), but not by the re-introduction of the Edr2 non-binding mutant of MK2, MK2/5 (0.4 and 0.2%). Taken together, this indicates that MK2–Edr2 interaction is essential for LSK repopulation capacity.

Discussion

MK2 is a downstream component of the p38 MAPK signalling cascade with pleiotropic functions. Acting as a protein kinase, MK2 controls the regulation of the actin cytoskeleton (Stokoe *et al*, 1992; Guay *et al*, 1997), stress-dependent small heat-shock protein phosphorylation (Vertii *et al*, 2006), and stability and translation of the AU-rich element containing cytokine mRNAs (Neininger *et al*, 2002; Hitti *et al*, 2006). Independently of its catalytic activity, MK2 stabilizes p38α (Kotlyarov *et al*, 2002) and could act as a shuttling protein, mediating nuclear export of p38α (Ben-Levy *et al*, 1998).

Here, we propose a new function for MK2 in maintaining HSC quiescence. This function involves MK2-targeting to PRC-1 through Edr1/2 binding and subsequent modulation of the transcriptional control mechanisms governing HSC

quiescence (summarized in Figure 7). This represents a mechanism for attracting signal-transducing protein kinases to specific target genes in mammalian cells as already described for the yeast, *S. cerevisiae* (Pokholok *et al*, 2006; Proft *et al*, 2006). We document the specific interaction of MK2 and members of PRC1 and define the regions involved in Edr2–MK2 interaction as a SAM domain on Edr2 and subdomains I–V in the small lobe of the kinase. The latter does not overlap with the p38α docking site on MK2, possibly allowing formation of a ternary complex.

Recently, the p38 MAPK pathway has been shown to control the lifespan of HSCs (Ito *et al*, 2006). Sustained

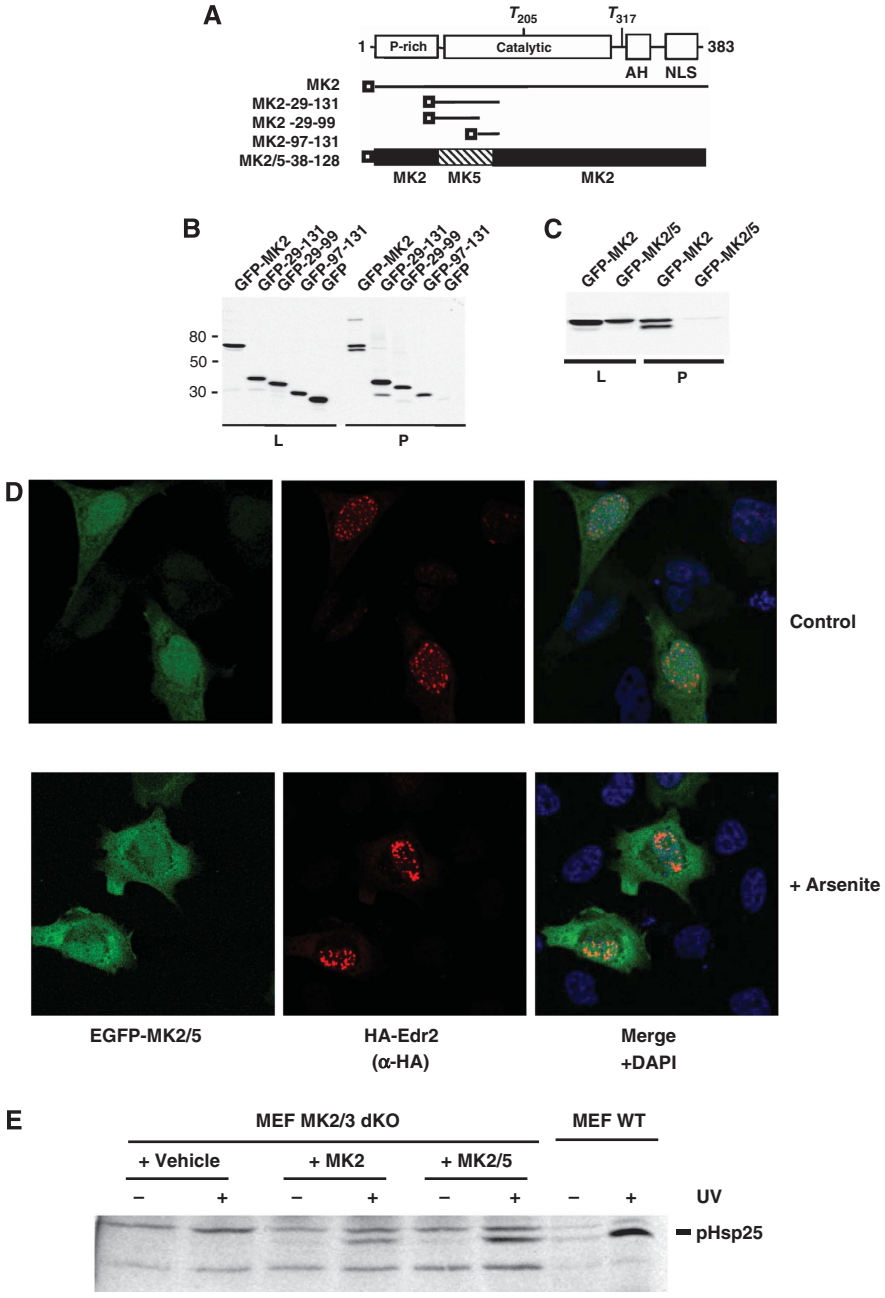

Figure 6 Identification of the Edr2-interacting region in MK2 and rescue of the repopulation capacity of MK2-deficient cells by MK2, but not by MK2/5. (**A**) Schematic representation of GFP–MK2, different GFP-tagged fragments of MK2, as well as an MK2/MK5 hybrid kinase (*P*-rich is the proline-rich N-terminal region, AH is the auto-inhibitory C-terminal helix containing the nuclear export signal (NES; Engel *et al*, 1998), NLS represents the nuclear localization signal and T205 and T317 are the regulatory phosphorylation sites of mouse MK2). (**B**, **C**) Lysates (*L*) from HEK 293 cells expressing the different GFP-tagged constructs described in (A) were subjected to GST-Edr2 pull-down (P). Proteins were detected by anti-GFP western blot. Molecular masses (kDa) are indicated in the left. (**D**) Comparable enzymatic activity of MK2 and MK2/5 against the *in vivo* substrate Hsp25 detected in transduced MEFs after UV stimulation (200 J/m^2) and 30 min recovery. (**E**) MK2/5 hybrid kinase misplaced from polycomb bodies (examined as in Figure 5B). (**F**) Competitive repopulation assay. 1×10^4 CD45.1+ LSK cells transduced with pMMP–IRES–GFP together with 1×10^4 CD45.2+ LSK cells transduced with the different bicistronic constructs indicated at the left were transplanted into recipient mice (CD45.1+) and analysed for repopulation capacity as described. Two characteristic experiments and statistical evaluation (right) ($N=6$) are shown. Asterisks indicate significant differences ($P<0.01$) to vehicle-transduced cells. Transfection efficiency (about 30% for all three constructs) was monitored by GFP-expression.

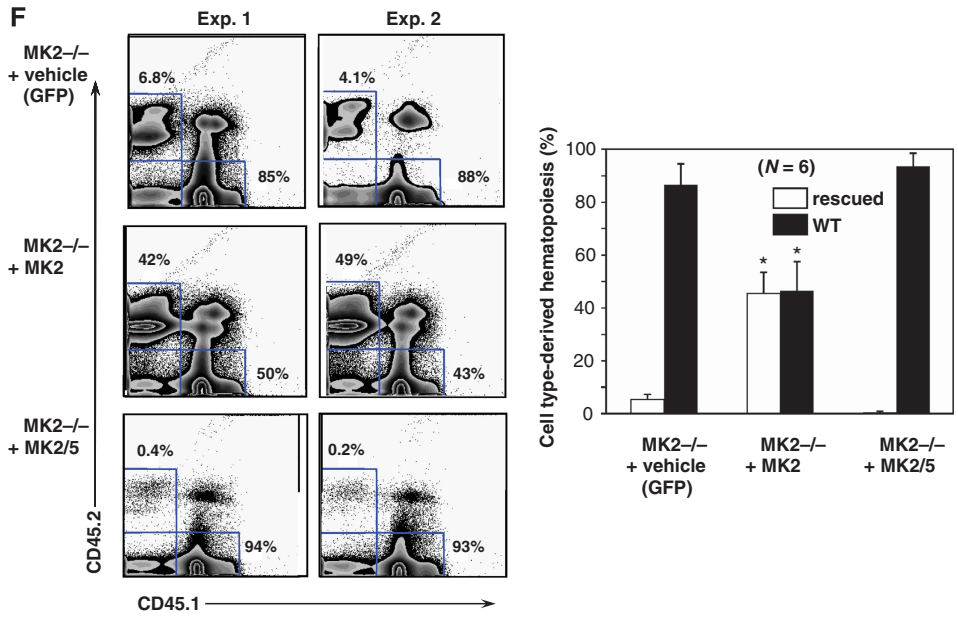

Figure 6 Continued.

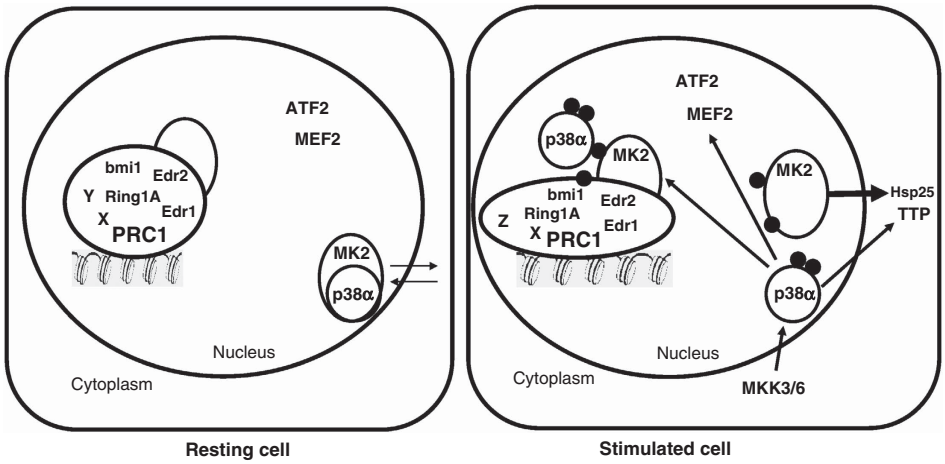

Figure 7 The model of stress -signalling to PRC1: In the nucleus of resting cells, a sub-population of MK2 (and MK3) is associated to PRC1 via specific interaction to Edr2 (and/or Edr1). A distinct, probably more abundant sub-population of MK2 (and MK3) exists in complex with p38α (or p38β). On stimulation of the p38 pathway, p38 is phosphorylated by MKK3 or MKK6 and, in turn, phosphorylates MK2 (and MK3). As a result of phosphorylation, the p38/MK2 complex becomes unstable (Lukas *et al*, 2004), the nuclear export signal of MK2 is unmasked (Neininger *et al*, 2001; White *et al*, 2007) and the sub-population of MK2 formerly bound to p38 is exported to the cytoplasm meeting its substrates such as Hsp25 and mRNA-binding proteins as tristetraprolin (TTP) (Hitti *et al*, 2006). Activated p38 may partially leave the nucleus (Ben-Levy *et al*, 1998), but also remains in the nucleus to phosphorylate transcription factors, such as ATF2 (Raingeaud *et al*, 1996) or MEF2 (Zhao *et al*, 1999), as well as PRC1-bound MK2/3. Activation of PRC-bound MK2/3 by p38 leads to phosphorylation of components of PRC1, such as Bmi1 (Voncken *et al*, 2005), and contributes to chromatin remodelling. Black balls symbolize phosphorylations.

activation of p38 MAPK under oxidative stress, which is probably paralleled by increased cytoplasmic accumulation of p38/MK2 complexes (Ben-Levy *et al*, 1998) and, hence, by their reduction at the PRC1, induces loss of 'stemness', similar to our findings in MK2-deficient mice. Thus, our analysis of MK2-deficient HSC may provide a missing link between the stress-induced MAPK pathway and Bmi1-controlled HSC maintenance.

It has been shown that the protein kinase MK3/3pK, which is closely related to MK2 and shows 75% identity in primary structure, is able to directly phosphorylate His-tagged Bmi1 *in vitro* at as yet unidentified sites (Voncken *et al*, 2005). In light of this observation, the MK2 could directly phosphorylate Bmi1 *in vivo*, as both enzymes share activators and substrates (Clifton *et al*, 1996; Ronkina *et al*, 2007).

Physiologically, we identified a new role for MK2 in maintaining HSC quiescence. Although we could show that the haematopoietic differentiation program seems to be intact in MK2-deficient cells, we identified a selective deficiency of the HSC compartment, as shown by decreased numbers of HSCs in MK2-deficient mice. Furthermore, we defined an increased fraction of proliferating cells in the early haematopoietic progenitor cell pool as well as increased *in vitro* proliferation, suggesting that MK2 is needed to put brakes on a state of quiescence by modulating the PRC1 complex. As a consequence of MK2 deficiency, 'stemness' is lost, as the

HSC's long-term engraftment and repopulation potential resides predominantly in the G0 fraction (Passegue, 2005). Mechanistically, we propose that targeting of the MK2 to PRC1 is responsible for the observed effects on HSCs. This idea is supported by our finding that the Edr2-binding domain of MK2 is necessary to rescue the repopulation capacity of MK2−/− LSK cells. Interestingly, it seems that the Edr2-non-binding mutant MK2/5 even suppresses repopulation capacity. We speculate that this could be because of the interference with MK3 action, which might, to a certain degree, functionally compensate for the loss of MK2. This idea is supported by the comparable expression of MK2- and MK3-mRNA in LSK cells (Supplementary Figure 10) and comparable Edr2-binding (Figure 4B) of both enzymes. However, a detailed analysis of the effects of the MK2/5 mutant in WT cells will be necessary to further substantiate this speculation.

Few extrinsic and intrinsic factors have been implicated in controlling HSC maintenance (Suda *et al*, 2005; Adams and Scadden, 2006). Bmi1, a component of PRC1, is a crucial molecule in governing 'stemness' of HSC (van der Lugt *et al*, 1994; Lessard and Sauvageau, 2003; Iwama *et al*, 2004) and neuronal stem cells (Molofsky *et al*, 2003). Interestingly, in contrast to Bmi1-deficient stem cells, the Ink4a locus as a downstream target of Bmi1 (Jacobs *et al*, 1999; Park *et al*, 2003), encoding p16Ink4a and p19Arf under the control of two distinct promoters (Quelle *et al*, 1995), is selectively affected in MK2-deficient HSC: Only the expression of p19Arf, a protein involved in p53-dependent apoptosis, is increased. The reason for this selectivity is currently unknown, but it might reflect the difference between Bmi1 deletion and loss of Bmi1 phosphorylation, or a different as-yet unknown function of MK2. Regardless of the molecular mechanism, MK2 emerges as a new important player and potential target to be manipulated in normal and malignant haematopoiesis.

Materials and methods

Mice

Mapkapk2^{tm1Mgl} mice (C57/Bl6) representing the conventional complete knockout of MK2 (Kotlyarov *et al*, 1999) were bred and maintained under specific pathogen-free conditions in the central animal facility at Hannover Medical School. In all experiments, age- and sex-matched mice were used at 4–12 weeks of age. All experiments were approved by the institutional review board.

Cell sorting and culture

For *in vitro* studies, purified SLAM (CD150+CD48−) or Lin$^-$Sca1$^+$c-kit$^+$ cells from MK2+/+ and MK2−/− mice were cultured in IMDM medium supplemented with 10% FCS, 2 mM L-glutamine, 1% penicillin–streptomycin, 1 mM non-essential amino acids, 10 ng/ml rm-IL3, 10 ng/ml rm-IL6, 50 ng/ml rm-SCF, 50 ng/ml and rh-Flt3L (all from Peprotech, Rocky Hill, NJ).

For *in vitro* proliferation experiments, LSK cells were cultured for 48 h as mentioned above and subsequently pulsed with 1 μCi ^{3}H-thymidine for 12 h. Incorporated ^{3}H-thymidine was quantified by scintillation counting.

For p38 inhibitor studies, Lin$^-$Sca1$^+$c-kit$^+$ cells from MK2+/+ mice were sorted and cultured either in the presence or in the absence of SB239063 (5 μM, Calbiochem) for 72 h.

For cell-cycle analysis, sorted LSK cells were cultured for 48 h *in vitro* and fixed with ice-cold absolute ethanol for 1 h on ice. Cells were washed, incubated with propidium iodide (0.5 μg/ml, Sigma) and RNase A (5 μg/ml, Qiagen) for 1 h, and analysed by flow cytometry.

Side population (SP) studies

SP studies were conducted as described earlier (Goodell *et al*, 1996). Briefly, RBC-depleted total bone marrow cells of MK2+/+ and MK2−/− mice were re-suspended in pre-warmed DMEM medium containing Hoechst 33342 dye (5 μg/ml, Sigma) either in the presence or in the absence of verapamil (50 μM, Sigma) and incubated for 90 min at 37°C. Cells were washed twice with ice-cold HBSS, stained with propidium iodide (2 μg/ml) and analysed by a Moflo cell sorter (DAKO Cytomation, Glostrup, Denmark).

Flow cytometry

Single cell suspensions were analysed by flow cytometry using FACS SCAN or FACS Canto and CELLQuest software, FACS Diva software (BD Biosciences) or FlowJo software (Tree Star, Inc., Ashland, OR). Cell sorting of defined sub-populations was carried out using the Moflo cell sorter with Summit software or FACSAria cell sorter (BD Biosciences). The following monoclonal antibodies (all from BD Pharmingen, San Diego, CA except noted otherwise) were used: CD3ε-biotin, CD-4-biotin, CD8-biotin, CD11b-biotin, CD11c-biotin, CD19-biotin, CD48-biotin (eBiosciences, San Diego, CA), CD117-APC, CD150-PE (eBiosciences), B220-biotin, Gr-1-biotin, Sca-1-PE and TER119-biotin.

BrdU incorporation

In vivo incorporation of BrdU into LSK cells was assessed using the FITC BrdU Flow kit (BD Pharmingen). After a single intraperitoneal injection of BrdU (Sigma, 1 mg per 6 g of mouse weight), an admixture of 1 mg/ml of BrdU was added to the drinking water for 3 days. Mice were killed, BM cells were prepared and stained with antibodies recognizing lineage, Scal and c-kit markers, and analysed by flow cytometry.

CFSE proliferation assay

For CFSE studies, purified CD150+CD48− cells were labeled with 2 mM CFSE (Molecular Probes, Karlsruhe, Germany) in IMDM complete medium at 37°C for 10 min. Cells were washed with PBS, cultured as indicated above and analysed by flow cytometry.

RNA isolation and real-time PCR

Total RNA was isolated using commercially available kit systems (Absolutely RNA mini prep kit,Stratagene, La Jolla, CA). cDNA was synthesized using oligo-dT primer and expand reverse transcriptase (Roche). p19 and p21 expression levels were determined by real-time PCR using the primers described in Supplementary data. The PCR reaction was carried out in duplicates using a LightCycler–FastStart DNA Master SYBR Green I kit (Roche) according to the manufacturer's instructions.

Competitive repopulation studies

Defined numbers of (i) RBC-depleted donor (CD45.2) BM or of (ii) LSK cells of 8-week-old MK2+/+ and MK2−/− mice or (iii) 10^4 MK2−/− LSK cells transduced with the bicistronic pMMP–IRES viral construct (see below) were mixed with (i) 10^5 competitor bone marrow or (ii) 10^4 competitor LSK cells or (iii) 10^4 LSK cells transduced with the viral GFP-expressing control construct (CD45.1) cells, respectively, and transplanted i.v. into lethally irradiated (10 Gy) congenic recipients (CD45.1). In the LSK repopulation experiments ((ii) and (iii)), 10^5 total-BM-compensatory carrier cells (CD45.1) were added to the cell mixture to create a supportive environment during the initial period after transplantation and to increase the viability of the transplanted animals. The number of stem cells in these compensatory cells is negligibly small compared with the number of stem cells in the LSK populations. Transplanted mice were maintained under specific pathogen-free conditions for 3 months. For secondary transplantation, 2×10^6 BM cells were transplanted into lethally irradiated congenic recipients and 12 weeks after transplantation, 2×10^6 BM cells were isolated, analysed for CD45.2 derived cells and subsequently transplanted into lethally irradiated congenic secondary recipients. At 16 weeks after transplantation, BM of secondary recipients was analysed for CD45.2-derived cells.

Yeast two-hybrid screen

A mouse-brain library (MY4008AH, MATCHMAKER, Clontech) in strain Y187 (MATα) was mated with pGBKT7-MK2 to identify the interaction partners of mouse MK2. About 2.5×10^7 colonies that contained 3.5×10^6 independent cDNA clones were screened.

Transfections, pull-down and co-immunoprecipitation

HEK293-T and HeLa cells were cultured and transfected as described (Schumacher *et al*, 2004). For *in vitro* pull-down assays, a total of 1×10^7 transfected HEK293-T cells expressing GST-tagged MK2, MK3, MK5 or Bmi1 were used and GST pull-down was carried out as described (Schumacher *et al*, 2004). Bound proteins were analysed by western blot using antibodies against Edr2 or Ring1B (Atsuta *et al*, 2001). Alternatively, purified recombinant hexahistidine-tagged Edr1, Edr2 or p38 proteins were incubated with recombinant GST or GST-tagged MK2 protein bound to glutathione Sepharose 4B beads. Binding of His-fusion proteins was detected by western blot using 6x-His antibodies (Clontech). For co-IP, 2×10^7 immortalized WT or MK2/3 double-knockout MEFs were lysed in 1.3 ml buffer (50 mM HEPES (pH 7.5), 1% Triton X-100, 10% glycerol, 150 mM NaCl, 1.5 mM $MgCl_2$, 1 mM EGTA). In all 2.5 mg of cell lysate was incubated with 5 μl of MK2 antibody (Cell Signaling3042) overnight at 4°C and subsequently incubated with 25 μl of protein G Sepharose (Amersham) for 1.5 h at 4°C. Beads were washed five times with cold lysis buffer and western blot was carried out using Edr2 antibody (Atsuta *et al*, 2001).

Gel filtration

In total, 4×10^7 immortalized WT or MK2−/− mouse embryonic fibroblasts (Kotlyarov *et al*, 1999) were lysed in 400 μl lysis buffer (20 mM HEPES pH 7.5, 50 mM KCl, 2 mM $MgCl_2$, 0.5% Nonidet P40, 0.5 mM DTT, protease inhibitor cocktail tablet (Roche Diagnostics)) and centrifued at 800 *g* for 8 min at 4°C. Supernatant was removed and the pelleted nuclei were lysed in Buffer A (50 mM HEPES pH 7.6, 250 mM NaCl, 10% glycerol, 0.5% Triton X-100, 1 mM EDTA, 1 mM DTT, protease inhibitor cocktail tablet (Roche Diagnostics)) for 20 min on ice. Nuclei were passed 10 times through a 20-gauge needle and centrifuged at 16 000 *g*, 4°C. In total, 500 μg of nuclear extract was separated by FPLC (LCC-500 Plus) using two Superose 6HR 30/10 columns connected in series (Pharmacia LKB Biotechnology, Uppsala, Sweden), developed with 0.05 M K_2HPO_4/KH_2PO_4, pH 7.2, 0.15M NaCl with a flow-rate of 0.1 ml/min. Proteins from fractions were precipitated by adding 1/100 volume of 2% deoxycholate, incubation for 30 min at 4°C and addition of 1/10 volume of 100% trichloroacetic acid. Samples were incubated overnight at 4°C, centrifuged for 15 min at 16 000 *g*, air-dried, dissolved in 4× SDS sample buffer and separated by 10% SDS–PAGE. Western blotting was carried out using anti-Ring1B (Atsuta *et al*, 2001) and anti-MK2 (Cell Signaling 3042) antibodies.

Fluorescence microscopy

For subcellular localization of YFP- and CFP-tagged proteins, the transfected cells (with lipofectamine/plus reagent, Invitrogen) were replated in chambered coverglass (Lab-Tek, Nunc) and analysed using a Leica DM IRBE microscope with the Leica TCS confocal systems program. For immunocytochemistry, HeLa cells were seeded on poly-L-lysine-coated coverslips. At 24 h after transfection of EGFP- and HA-tagged proteins, cells were fixed with 4% paraformaldehyde and incubated overnight with HA antibodies (Santa Cruz, sc-805) followed by Alexa 555 (Invitrogen, A31572) staining.

Cloning, construction of deletion mutants and site-directed mutagenesis

Cloning techniques are described in detail in Supplementary data. For generation of deletion mutants, the fusion of amino acids 29–131, 29–99 and 97–131 of MK2 to EGFP was carried out by inserting *Eco*RI–*Bam*HI-cut PCR fragments, amplified from pEGFP-MK2 (Engel *et al*, 1995) using the primers given in Supplementary data, into pEGFP-C1 (Clontech). The pEGFP–MK2/MK5 hybrid was generated by deletion of MK2-amino acids 37–131 from pEGFP–MK2 using *Pst*I/*Sac*I and cloning of *Pst*I–*Sac*I-cut PCR fragment of MK5-amino acid 10–110, amplified with the primers given in Supplementary data.

Viral transductions of MEFs and L-negative cells

MEFs were tranduced with the retroviral constructs pMMP–IRES–GFP, pMMP–MK2–IRES–GFP and pMMP–MK2/5–IRES–GFP as described (Ronkina *et al*, 2007). pHsp25 was detected by western blotting using an anti-phosphoS86-Hsp25 antibody (BioSource). Before retroviral transduction, L-negative cells were stimulated with mSCF (100 ng/ml), hIL-11 (100 ng/ml) and hFlt3-Lig (100 ng/ml) for 48 h in StemSpan. Lin(−) Ly 5.1 cells were transduced with pMMP–IRES–GFP (MOI = 3) whereas Lin(−) Ly 5.2 were transduced with the different retroviral transfer vectors with MOI = 3 after 48 and 60 h. The Lin(−) transduced cells were sorted for Sca-1$^+$c-Kit$^+$LSK before mixing for repopulation assay.

Supplementary data

Further experimental data, data about plasmids and primers used for cloning and PCR as well as cloning details are provided in the Supplementary data. Supplementary Figures are provided. Supplementary data are available at *The EMBO Journal* Online (http://www.embojournal.org).

Acknowledgements

We thank David Luckhaus and Cosima Hakim for help with the initial two-hybrid screen and with the gel filtration experiments, respectively. Dr Matthias Ballmaier and the central cell-sorting facility at MHH are greatly acknowledged. This work was supported by grants from DFG SFB 566 and DFG KliFo 110.

References

Adams GB, Scadden DT (2006) The hematopoietic stem cell in its place. *Nat Immunol* **7:** 333–337

Atsuta T, Fujimura S, Moriya H, Vidal M, Akasaka T, Koseki H (2001) Production of monoclonal antibodies against mammalian Ring1B proteins. *Hybridoma* **20:** 43–46

Ben-Levy R, Hooper S, Wilson R, Paterson HF, Marshall CJ (1998) Nuclear export of the stress-activated protein kinase p38 mediated by its substrate MAPKAP kinase-2. *Curr Biol* **8:** 1049–1057

Blank U, Karlsson G, Moody JL, Utsugisawa T, Magnusson M, Singbrant S, Larsson J, Karlsson S (2006) Smad7 promotes self-renewal of hematopoietic stem cells. *Blood* **108:** 4246–4254

Boyer LA, Plath K, Zeitlinger J, Brambrink T, Medeiros LA, Lee TI, Levine SS, Wernig M, Tajonar A, Ray MK, Bell GW, Otte AP, Vidal M, Gifford DK, Young RA, Jaenisch R (2006) Polycomb complexes repress developmental regulators in murine embryonic stem cells. *Nature* **441:** 349–353

Cheng T, Rodrigues N, Shen H, Yang Y, Dombkowski D, Sykes M, Scadden DT (2000) Hematopoietic stem cell quiescence maintained by p21cip1/waf1. *Science* **287:** 1804–1808

Clifton AD, Young PR, Cohen P (1996) A comparison of the substrate specificity of MAPKAP kinase-2 and MAPKAP kinase-3 and their activation by cytokines and cellular stress. *FEBS Lett* **392:** 209–214

Duncan AW, Rattis FM, DiMascio LN, Congdon KL, Pazianos G, Zhao C, Yoon K, Cook JM, Willert K, Gaiano N, Reya T (2005) Integration of Notch and Wnt signaling in hematopoietic stem cell maintenance. *Nat Immunol* **6:** 314–322

Engel K, Kotlyarov A, Gaestel M (1998) Leptomycin B-sensitive nuclear export of MAPKAP kinase 2 is regulated by phosphorylation. *EMBO J* **17:** 3363–3371

Engel K, Schultz H, Martin F, Kotlyarov A, Plath K, Hahn M, Heinemann U, Gaestel M (1995) Constitutive activation of mitogen-activated protein kinase-activated protein kinase 2 by mutation of phosphorylation sites and an A-helix motif. *J Biol Chem* **270:** 27213–27221

Gaestel M (2006) MAPKAP kinases—MKs—two's company, three's a crowd. *Nat Rev Mol Cell Biol* **7:** 120–130

Goodell MA, Brose K, Paradis G, Conner AS, Mulligan RC (1996) Isolation and functional properties of murine hematopoietic stem cells that are replicating *in vivo*. *J Exp Med* **183:** 1797–1806

Guay J, Lambert H, Gingras-Breton G, Lavoie JN, Huot J, Landry J (1997) Regulation of actin filament dynamics by p38 map kinase-mediated phosphorylation of heat shock protein 27. *J Cell Sci* **110:** 357–368

Hegen M, Gaestel M, Nickerson-Nutter CL, Lin LL, Telliez JB (2006) MAPKAP kinase 2-deficient mice are resistant to collagen-induced arthritis. *J Immunol* **177:** 1913–1917

Hitti E, Iakovleva T, Brook M, Deppenmeier S, Gruber AD, Radzioch D, Clark AR, Blackshear PJ, Kotlyarov A, Gaestel M (2006) Mitogen-activated protein kinase-activated protein kinase 2 regulates tumor necrosis factor mRNA stability and translation mainly by altering tristetraprolin expression, stability, and binding to adenine/uridine-rich element. *Mol Cell Biol* **26:** 2399–2407

Hock H, Hamblen MJ, Rooke HM, Schindler JW, Saleque S, Fujiwara Y, Orkin SH (2004) Gfi-1 restricts proliferation and preserves functional integrity of haematopoietic stem cells. *Nature* **431:** 1002–1007

Isono K, Fujimura Y, Shinga J, Yamaki M, O-Wang J, Takihara Y, Murahashi Y, Takada Y, Mizutani-Koseki Y, Koseki H (2005) Mammalian polyhomeotic homologues Phc2 and Phc1 act in synergy to mediate polycomb repression of Hox genes. *Mol Cell Biol* **25:** 6694–6706

Ito K, Hirao A, Arai F, Takubo K, Matsuoka S, Miyamoto K, Ohmura M, Naka K, Hosokawa K, Ikeda Y, Suda T (2006) Reactive oxygen species act through p38 MAPK to limit the lifespan of hematopoietic stem cells. *Nat Med* **12:** 446–451

Iwama A, Oguro H, Negishi M, Kato Y, Morita Y, Tsukui H, Ema H, Kamijo T, Katoh-Fukui Y, Koseki H, van Lohuizen M, Nakauchi H (2004) Enhanced self-renewal of hematopoietic stem cells mediated by the polycomb gene product Bmi-1. *Immunity* **21:** 843–851

Jacobs JJ, Kieboom K, Marino S, DePinho RA, van Lohuizen M (1999) The oncogene and Polycomb-group gene bmi-1 regulates cell proliferation and senescence through the ink4a locus. *Nature* **397:** 164–168

Jagavelu K, Tietge UJ, Gaestel M, Drexler H, Schieffer B, Bavendiek U (2007) Systemic deficiency of the MAP kinase activated protein kinase 2 reduces atherosclerosis in hypercholesterolemic mice. *Circ Res* **101:** 1104–1112

Kiel MJ, Yilmaz OH, Iwashita T, Terhorst C, Morrison SJ (2005) SLAM family receptors distinguish hematopoietic stem and progenitor cells and reveal endothelial niches for stem cells. *Cell* **121:** 1109–1121

Kirito K, Fox N, Kaushansky K (2003) Thrombopoietin stimulates Hoxb4 expression: an explanation for the favorable effects of TPO on hematopoietic stem cells. *Blood* **102:** 3172–3178

Kotlyarov A, Neininger A, Schubert C, Eckert R, Birchmeier C, Volk HD, Gaestel M (1999) MAPKAP kinase 2 is essential for LPS-induced TNF-alpha biosynthesis. *Nat Cell Biol* **1:** 94–97

Kotlyarov A, Yannoni Y, Fritz S, Laass K, Telliez JB, Pitman D, Lin LL, Gaestel M (2002) Distinct cellular functions of MK2. *Mol Cell Biol* **22:** 4827–4835

Lessard J, Sauvageau G (2003) Bmi-1 determines the proliferative capacity of normal and leukaemic stem cells. *Nature* **423:** 255–260

Levine SS, King IF, Kingston RE (2004) Division of labor in polycomb group repression. *Trends Biochem Sci* **29:** 478–485

Lukas SM, Kroe RR, Wildeson J, Peet GW, Frego L, Davidson W, Ingraham RH, Pargellis CA, Labadia ME, Werneburg BG (2004) Catalysis and function of the p38 alpha.MK2a signaling complex. *Biochemistry* **43:** 9950–9960

Lund AH, van Lohuizen M (2004) Polycomb complexes and silencing mechanisms. *Curr Opin Cell Biol* **16:** 239–246

Molofsky AV, Pardal R, Iwashita T, Park IK, Clarke MF, Morrison SJ (2003) Bmi-1 dependence distinguishes neural stem cell self-renewal from progenitor proliferation. *Nature* **425:** 962–967

Neininger A, Kontoyiannis D, Kotlyarov A, Winzen R, Eckert R, Volk HD, Holtmann H, Kollias G, Gaestel M (2002) MK2 targets AU-rich elements and regulates biosynthesis of tumor necrosis factor and interleukin-6 independently at different post-transcriptional levels. *J Biol Chem* **277:** 3065–3068

Neininger A, Thielemann H, Gaestel M (2001) FRET-based detection of different conformations of MK2. *EMBO Rep* **2:** 703–708

Ohta H, Sawada A, Kim JY, Tokimasa S, Nishiguchi S, Humphries RK, Hara J, Takihara Y (2002) Polycomb group gene rae28 is required for sustaining activity of hematopoietic stem cells. *J Exp Med* **195:** 759–770

Park IK, Qian D, Kiel M, Becker MW, Pihalja M, Weissman IL, Morrison SJ, Clarke MF (2003) Bmi-1 is required for maintenance of adult self-renewing haematopoietic stem cells. *Nature* **423:** 302–305

Passegue E (2005) Hematopoietic stem cells, leukemic stem cells and chronic myelogenous leukemia. *Cell Cycle* **4:** 266–268

Platanias LC (2003) Map kinase signaling pathways and hematologic malignancies. *Blood* **101:** 4667–4679

Pokholok DK, Zeitlinger J, Hannett NM, Reynolds DB, Young RA (2006) Activated signal transduction kinases frequently occupy target genes. *Science* **313:** 533–536

Proft M, Mas G, de Nadal E, Vendrell A, Noriega N, Struhl K, Posas F (2006) The stress-activated Hog1 kinase is a selective transcriptional elongation factor for genes responding to osmotic stress. *Mol Cell* **23:** 241–250

Qiao F, Bowie JU (2005) The many faces of SAM. *Sci STKE* **2005:** re7

Quelle DE, Zindy F, Ashmun RA, Sherr CJ (1995) Alternative reading frames of the INK4a tumor suppressor gene encode two unrelated proteins capable of inducing cell cycle arrest. *Cell* **83:** 993–1000

Raingeaud J, Whitmarsh AJ, Barrett T, Derijard B, Davis RJ (1996) MKK3- and MKK6-regulated gene expression is mediated by the p38 mitogen-activated protein kinase signal transduction pathway. *Mol Cell Biol* **16:** 1247–1255

Rajasekhar VK, Begemann M (2007) Concise review: roles of polycomb group proteins in development and disease: a stem cell perspective. *Stem Cells* **25:** 2498–2510

Reya T, Duncan AW, Ailles L, Domen J, Scherer DC, Willert K, Hintz L, Nusse R, Weissman IL (2003) A role for Wnt signalling in self-renewal of haematopoietic stem cells. *Nature* **423:** 409–414

Ronkina N, Kotlyarov A, Dittrich-Breiholz O, Kracht M, Hitti E, Milarski K, Askew R, Marusic S, Lin LL, Gaestel M, Telliez JB (2007) The mitogen-activated protein kinase (MAPK)-activated protein kinases MK2 and MK3 cooperate in stimulation of tumor necrosis factor biosynthesis and stabilization of p38 MAPK. *Mol Cell Biol* **27:** 170–181

Schumacher S, Laass K, Kant S, Shi Y, Visel A, Gruber AD, Kotlyarov A, Gaestel M (2004) Scaffolding by ERK3 regulates MK5 in development. *EMBO J* **23:** 4770–4779

Stokoe D, Engel K, Campbell DG, Cohen P, Gaestel M (1992) Identification of MAPKAP kinase 2 as a major enzyme responsible for the phosphorylation of the small mammalian heat shock proteins. *FEBS Lett* **313:** 307–313

Suda T, Arai F, Hirao A (2005) Hematopoietic stem cells and their niche. *Trends Immunol* **26:** 426–433

Suzuki M, Mizutani-Koseki Y, Fujimura Y, Miyagishima H, Kaneko T, Takada Y, Akasaka T, Tanzawa H, Takihara Y, Nakano M, Masumoto H, Vidal M, Isono K, Koseki H (2002) Involvement of the Polycomb-group gene Ring1B in the specification of the anterior-posterior axis in mice. *Development* **129:** 4171–4183

Tamura K, Sudo T, Senftleben U, Dadak AM, Johnson R, Karin M (2000) Requirement for p38alpha in erythropoietin expression: a role for stress kinases in erythropoiesis. *Cell* **102:** 221–231

Tanoue T, Adachi M, Moriguchi T, Nishida E (2000) A conserved docking motif in MAP kinases common to substrates, activators and regulators. *Nat Cell Biol* **2:** 110–116

Valk-Lingbeek ME, Bruggeman SW, van Lohuizen M (2004) Stem cells and cancer; the polycomb connection. *Cell* **118:** 409–418

van der Lugt NM, Domen J, Linders K, van Roon M, Robanus-Maandag E, te Riele H, van der Valk M, Deschamps J, Sofroniew M, van Lohuizen M, Berns A (1994) Posterior transformation, neurological abnormalities, and severe hematopoietic defects in mice with a targeted deletion of the bmi-1 proto-oncogene. *Genes Dev* **8:** 757–769

Vertii A, Hakim C, Kotlyarov A, Gaestel M (2006) Analysis of properties of small heat shock protein Hsp25 in MAPK-activated protein kinase 2 (MK2)-deficient cells: MK2-dependent insolubilization of Hsp25 oligomers correlates with susceptibility to stress. *J Biol Chem* **281:** 26966–26975

Voncken JW, Niessen H, Neufeld B, Rennefahrt U, Dahlmans V, Kubben N, Holzer B, Ludwig S, Rapp UR (2005) MAPKAP kinase 3pK phosphorylates and regulates chromatin association of the polycomb group protein Bmi1. *J Biol Chem* **280:** 5178–5187

White A, Pargellis CA, Studts JM, Werneburg BG, Farmer II BT (2007) Molecular basis of MAPK-activated protein kinase 2:p38 assembly. *Proc Natl Acad Sci USA* **104:** 6353–6358

Winzen R, Kracht M, Ritter B, Wilhelm A, Chen CY, Shyu AB, Muller M, Gaestel M, Resch K, Holtmann H (1999) The p38 MAP kinase pathway signals for cytokine-induced mRNA stabilization via MAP kinase-activated protein kinase 2 and an AU-rich region-targeted mechanism. *EMBO J* **18:** 4969–4980

Yamaki M, Isono K, Takada Y, Abe K, Akasaka T, Tanzawa H, Koseki H (2002) The mouse Edr2 (Mph2) gene has two forms of mRNA encoding 90- and 36-kDa polypeptides. *Gene* **288:** 103–110

Yannoni YM, Gaestel M, Lin LL (2004) P66(ShcA) interacts with MAPKAP kinase 2 and regulates its activity. *FEBS Lett* **564:** 205–211

Zhao M, New L, Kravchenko VV, Kato Y, Gram H, di Padova F, Olson EN, Ulevitch RJ, Han J (1999) Regulation of the MEF2 family of transcription factors by p38. *Mol Cell Biol* **19:** 21–30

Zink B, Paro R (1989) *In vivo* binding pattern of a trans-regulator of homoeotic genes in Drosophila melanogaster. *Nature* **337:** 468–471